European Journal of Control 59 (2021) 250–263

Contents lists available at ScienceDirect

European Journal of Control

journal homepage: www.elsevier.com/locate/ejcon

Tuning rules for unstable dead-time processes

Rejane C. Sá Rodrigues, Andresa K.R. Sombra*, Bismark C. Torrico, René D.O. Pereira, Marcus D.do N. Forte, Magno P. de Almeida Filho, Fabrício G. Nogueira

Department of Electrical Engineering, Federal University of Ceará, Fortaleza 60455-760, CE, Brazil

ARTICLE INFO

Article history:
Received 6 December 2019
Revised 3 October 2020
Accepted 15 October 2020
Available online 28 October 2020

Recommended by Prof. T Parisini

Keywords:
Dead-time compensator
Sampling period
Robustness
Time-delay systems
Unstable process

ABSTRACT

Despite many advances in the field of dead-time compensators (DTCs) for unstable first-order plus dead-time (UFOPDT) processes, the tuning, in general, is manually carried out. Therefore, this paper proposes simple tuning rules for a DTC intended to UFOPDT processes. The rules are based on the relative dead time, desired closed-loop time constant, and achievable robustness. Besides, as the practical implementation is always in the discrete-time domain, a method to choose the sampling period for UFOPDT processes is presented. Four simulation examples from the literature are used to show the advantages of the proposed method. In addition, an experiment with a propeller pendulum is performed to confirm such advantages in the control of a real unstable process with dead time.

1. Introduction

Several application fields in industry, such as chemistry, aviation, among others, present a significant dead time and unstable open-loop behavior [2,30]. For this class of systems, the closed-loop performance can be improved significantly using controllers that incorporate the dead-time process model in its structure to predict the process output. The predictor is used to compensate the dead-time by avoiding the appearance of the time-delay in the characteristic equation, simplifying the tuning of the controller. These kinds of controllers are also known as dead-time compensators (DTCs) [22]. One of the first and most widespread DTCs in literature was the Smith predictor (SP) proposed in 1957 [29]. However, it presents some drawbacks and can not be used properly for integrating and unstable open-loop processes [21,22]. Over the years, Smith's idea has been refined and turned possible to apply the DTCs not only to integrative or unstable open-loop processes [13,39], but predictive structures have also been incorporated into more complex systems, which consider event-triggered control [5,16] and linear parameter-varying (LPV) approaches [20].

In [13], it was proposed a DTC structure for stable, unstable, and integrative processes. The structure is based on an observer used to predict the process output and estimate the input disturbance. The control input is computed based on the estimated disturbance and the output prediction using a proportional controller, therefore, avoiding windup effects. It is also proposed a particular solution for dead-beat response. In [1,3,4,28,38], it was presented a DTC structure, namely the Generalized Predictor (GP), whose main idea is to estimate the undelayed output in order to design a controller focusing on disturbance rejection. Another DTC was the filtered SP (FSP) [23,27], where a primary controller is tuned to deal with set-point tracking and a filter to deal with stability, robustness and disturbance rejection.

In [8,9], it was presented a modified FSP for first-order-plus-dead-time (FOPDT) models, with a proportional gain as the primary controller instead of a traditional proportional-integral (PI) controller, namely P-FSP. In these two works, it was shown, by means of simulations, that this control structure deals better with the problem of plants with saturating actuators, simplifying their treatment. In [11,12,40], comparisons with the FSP where made by means of a series of experiments, confirming that the attractiveness of the P-FSP is not restricted just to the case of constrained control. In [6] the formulation of the P-FSP was extended for integrating-plus-dead-time (IPDT) processes. In [7], it was proposed a new implementation structure for the P-FSP to better deal with IPDT processes and, by means of experiments, a comparison to a filtered PI controller was made, obtaining in constrained control better performance and robustness.

The works [31,32,34] proposed simplified versions of the FSP, with lower-order controllers compared to the traditional version

* Corresponding author.
E-mail addresses: rejane_sa@ifce.edu.br (R.C. Sá Rodrigues), andresasombra@dee.ufc.br (A.K.R. Sombra), bismark@dee.ufc.br (B.C. Torrico), reneolimpio@alu.ufc.br (R.D.O. Pereira), davi2812@dee.ufc.br (M.D.d.N. Forte), magnoprudencio@alu.ufc.br (M.P.d.A. Filho), fnogueira@dee.ufc.br (F.G. Nogueira).

https://doi.org/10.1016/j.ejcon.2020.10.001
0947-3580/

and equivalent or better robustness and disturbance rejection response.

For the aforementioned works tuning procedures are required for each particular system. On the other hand, tuning rules approach allows the control engineer to obtain the controller adjustment directly from plant parameters.

When controlling unstable processes with dead time, an important step with any controller is the tuning. A well-tuned controller can achieve both satisfactory performance and robustness. A simple way to achieve that is by means of a tuning rule. Employing an analytic tuning rule, instead of being tuned for a particular case, the controller can be tuned considering a general case. Therefore, proposing a tuning rule to adjust the controller is valuable to simplify the tuning process and to make it easier the use in the industry.

In this work, a tuning rule is considered a mathematical expression used to compute controller tuning parameters. It can be based on model parameters, and desired performance and robustness specifications. There are in the literature only a few works that proposed tuning rules for controllers that deal with unstable first-order-plus-dead-time (UFOPDT) processes. Most of them were proposed for PI and PID controllers [18,19,25,36]. It is unusual to find works proposing tuning rules for DTCs. An automatic tuning procedure for a DTC scheme, using tuning rules based on optimization results, was presented in [24].

Even though the practical implementation of DTCs is in the discrete-time domain, the aforementioned works do not study the over or undersampling effect. For some industrial applications, it is highly necessary to save network and computational resources [17]. Therefore, the ideal sampling period for control structures would be the biggest one that does not significantly affect the performance and robustness of the control system [35]. Furthermore, to simplify the design, analytic rules should be available to adjust the controller according to not only a desired robustness level, but also to the process sampling period.

Although many solutions to compensate dead-time have been presented in the last years, in some cases, the performance of the closed-loop response presents similar or equivalent results. Therefore, what leads to the choice of one desired strategy is the simplicity of the control structure and its tuning. Furthermore, tuning rules techniques often require easy-to-tune controllers based on simple models, like UFOPDT models. One of the controllers in the literature that satisfy these requirements is the simplified DTC (SDTC), also known as simplified FSP (SFSP) [33]. Its adoption in this work is justified by: (i) it presents fewer tuning parameters than the FSP [31], (ii) it can be directly extended to state-space models and the implementation of the predictor does not need an explicit pole-zero cancellation when dealing with integrating or unstable processes [32] and, (iii) even though processes with saturation are not the focus of this work, it presents good performance for the case of saturating actuators just by adding the saturation model at the input of the process model, as widely studied in [8,9,11,12,15,40]. However, this characteristic does no hold for a simplified control structure in a 2-DOF scheme.

Therefore, in this context, the main contributions of this work are: (i) a tuning rule for a DTC, using UFOPDT models, based on the maximum achievable robustness to dead-time uncertainties, in order to achieve a desired robustness and (ii) an analytic rule for choosing the sampling period maintaining the robust stability condition obtained by the tuning rule. Furthermore, to the knowledge of the authors, the contributions of this manuscript are original and have not been published in any other work in the literature.

The content of this paper is divided into eight sections, as follows. Section 1 is the introduction. In Section 2, the SDTC is described in order to present the controller base structure for the strategy proposed in this paper. The maximum achievable uncertainty of dead-time is also addressed in Section 3. The procedure for obtaining a rule to tune the robustness filter pole is shown in Section 4. Meanwhile, the analysis of the sampling period is provided in Section 5. The simulation results are presented in Section 6. Experimental results in a propeller pendulum plant are presented in Section 7. The paper ends with the conclusions in Section 8.

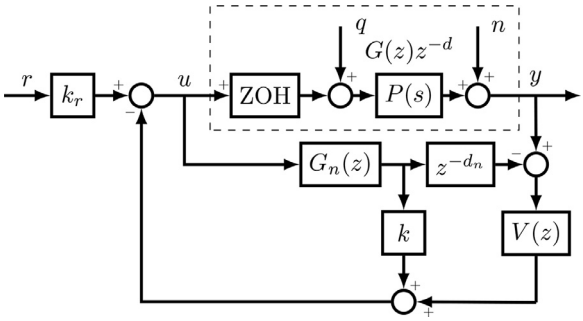

Fig. 1. The conceptual SDTC control structure.

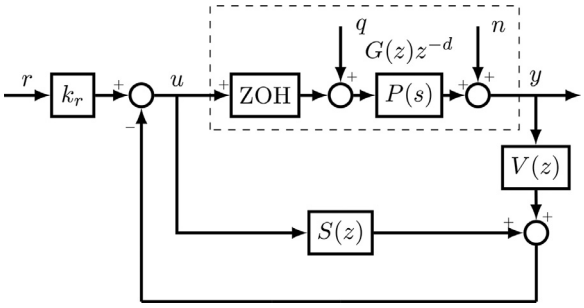

Fig. 2. Implementation control structure of the SDTC.

2. The simplified dead-time compensator

The conceptual structure of the SDTC when using FOPDT models is presented in Fig. 1, where $G_n(z)$ is the delay free nominal process model, $P(z)$ represents the real process, d_n is the nominal dead time, k_r and k are gains and $V(z)$ is the robustness filter. It is important o highlight that the conceptual structure of the SDTC is used only for design purposes because it presents an unstable mode corresponding to the plant pole, which produces internal stability problems.

The nominal process model $P_n(z) = G_n(z)z^{-d_n}$ can be represented by

$$P_n(z) = \frac{b_0 z^{-1}}{1 - a_1 z^{-1}} z^{-d_n}, \tag{1}$$

where $0 < a_1 < 1$ for stable processes and $a_1 > 1$ for unstable processes.

In the nominal case, it is considered that the nominal process model represents with fidelity the process $(P(z) = P_n(z))$. Aiming to analyse controller properties, the closed-loop transfer functions and the condition for robust stability are obtained for the nominal case.

$$H_{yr}(z) = \frac{Y(z)}{R(z)} = \frac{k_r P_n(z)}{1 + kG_n(z)}, \tag{2}$$

$$H_{yq}(z) = \frac{Y(z)}{Q(z)} = P_n(z)\left[1 - \frac{P_n(z)V(z)}{1 + kG_n(z)}\right], \tag{3}$$

$$H_{un}(z) = \frac{U(z)}{N(z)} = \frac{-V(z)}{1 + kG_n(z)}, \tag{4}$$

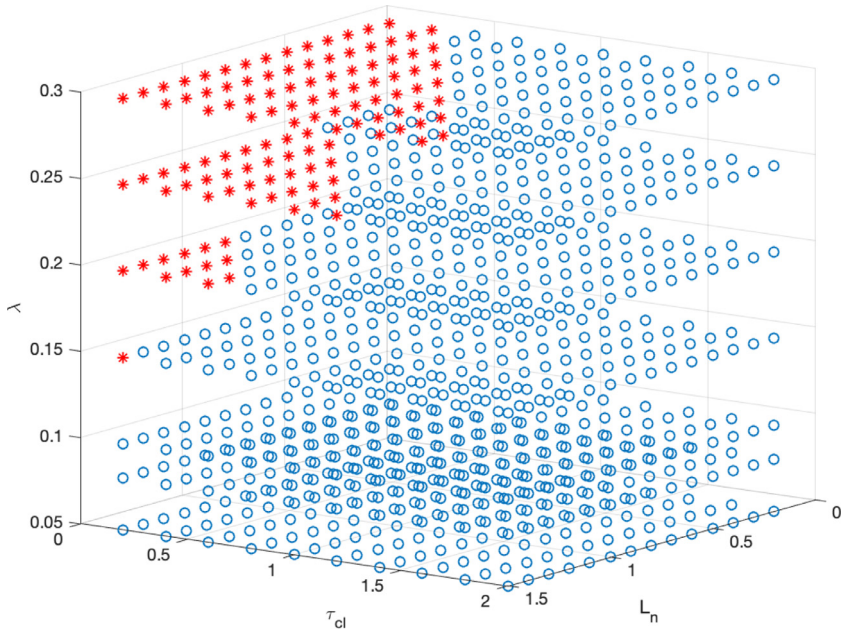

Fig. 3. Comparison between the data with results stable and unstable $\hat{\alpha}_c$.

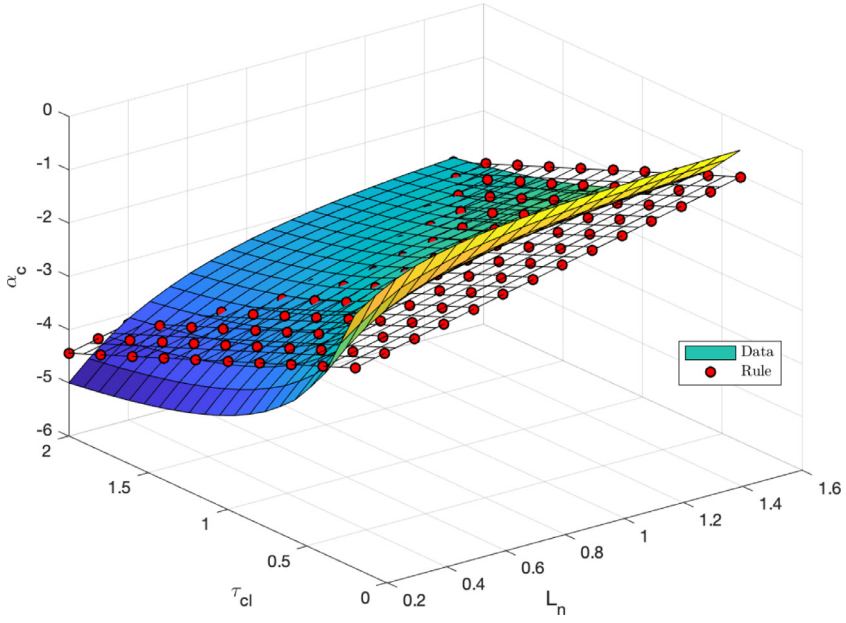

Fig. 4. Comparison between the data and the rule ($\lambda = 0.1$).

$$I_r(\omega) = \left| \frac{1 + kG_n(z)}{V(z)P_n(z)} \right|_{z=e^{j\omega T_s}} > \delta P(\omega). \tag{5}$$

In the above expressions, $R(z)$, $U(z)$, $N(z)$, $Y(z)$ and $Q(z)$ are Z-transforms of the following signals, respectively: set-point, control action, measurement noise, process output, and input load disturbance; $H_{yr}(z)$, $H_{yq}(z)$, and $H_{un}(z)$ are the transfer functions of the closed-loop system. $I_r(\omega)$ is defined as robustness index, the norm-bound of the multiplicative uncertainty term is $\delta P(\omega)$ and T_s is the sampling period frequency range at $0 < \omega < \pi/T_s$.

The SDTC tuning is made in two steps: the tuning for set-point tracking and the tuning for load disturbance rejection.

Firstly, the gains k and k_r are tuned using (2) to place a desired pole for set-point tracking performance. This is accomplished by making

$$H_{yr}(z) = \frac{(1 - a_c)z^{-1}}{1 - a_c z^{-1}} z^{-dn}, \tag{6}$$

where (6) is the desired closed-loop transfer function. As a result of this equality, it is obtained

$$k = \frac{a_1 - a_c}{b_0}, \tag{7}$$

$$k_r = \frac{1 - a_c}{b_0}. \tag{8}$$

Finally, once k_r and k are known, the robustness filter $V(z)$ is designed to stabilize the predictor and to reject disturbances at steady state. To be able to satisfy both conditions, $V(z)$ requires at least two coefficients on its numerator. Therefore, it is written

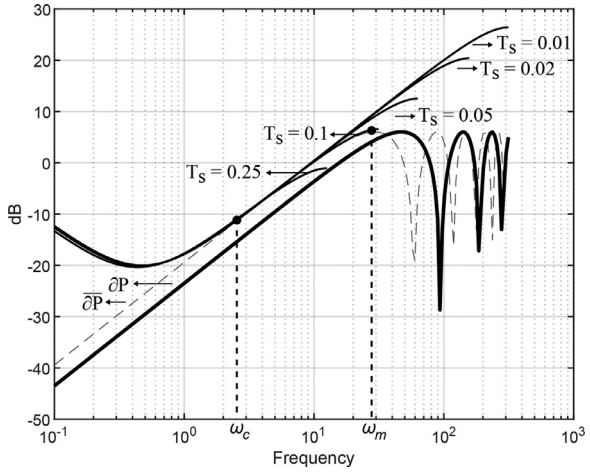

Fig. 5. Robustness Indexes for system (36) with $L = 1.5$.

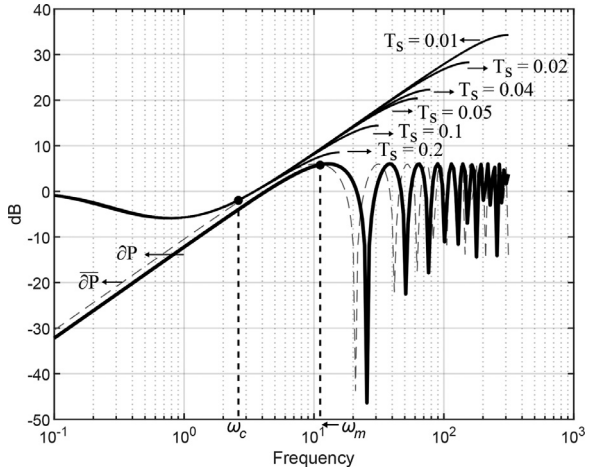

Fig. 6. Robustness Indexes for system (36) with $L = 0.2$.

as

$$V(z) = \frac{v_0 + v_1 z^{-1}}{1 - \beta z^{-1}}, \tag{9}$$

where β is a tuning parameter.

Also, to meet conditions (i) and (ii), it is necessary, respectively, that

$$\begin{aligned} &H_{yq}(z)|_{z=1} = 0, \\ &H_{yq}(z)|_{z=a_1} = 0. \end{aligned} \tag{10}$$

This is, respectively, equivalent to

$$\begin{aligned} &V(1) = k_r, \\ &k - V(a_1)a_1^{-dn} = 0. \end{aligned} \tag{11}$$

These expressions result in the following system of equations:

$$\begin{aligned} &v_0 + v_1 = k_r(1-\beta) \\ &v_0 + \frac{v_1}{a_1} = k\left(1 - \frac{\beta}{a_1}\right)a_1^{d_n}, \end{aligned} \tag{12}$$

from where one can obtain the values of v_0 and v_1 as

$$v_0 = \frac{1}{1-a_1}[k_r(1-\beta) - k(a_1-\beta)a_1^{d_n}], \tag{13}$$

$$v_1 = \frac{1}{1-a_1}[-a_1 k_r(1-\beta) + k(a_1-\beta)a_1^{d_n}]. \tag{14}$$

2.1. Implementation control structure

The implementation structure of the SDTC is shown in Fig. 2 where the transfer function $S(z)$ is given by

$$S(z) = \frac{b_0 z^{-1}}{1 - a_1 z^{-1}}\left(k - \frac{v_0 + v_1 z^{-1}}{1 - \beta z^{-1}} z^{-d}\right). \tag{15}$$

Note that the undesired pole of the process $z = a_1$ appears in the above expression, making the resulting closed-loop system internally unstable. In [23], a pole-zero cancellation method was used to avoid this problem. In a later work [32], another solution was proposed for unstable processes in the continuous-time domain that can also be applied to the discrete-time domain. It is important to mention that the conceptual structure of the FSP, shown in Fig. 1, cannot be used in practice because it presents some unobservable modes. However, this structure is useful for control design, allowing to easily find conditions to deal with stable, integrative, and unstable dead-time processes. The implementation structure, shown in Fig. 2, is free of unobservable modes and should be used in practice.

By using partial fractions decomposition for $\beta \neq a_1$ and conditions (11), $S(z)$ can be rewritten as

$$S(z) = \frac{b_0 k z^{-1}}{1 - a_1 z^{-1}} - \frac{b_0 k a_1^d z^{-d-1}}{1 - a_1 z^{-1}} + \frac{B z^{-d}}{1 - \beta z^{-1}}, \tag{16}$$

where $B = b_0(\beta v_0 + v_1)/(\beta - a_1)$.

By applying long division in the first term of (16), $S(z)$ results

$$S(z) = \sum_{i=1}^{d} k a_1^{i-1} b_0 z^{-i} + \frac{B}{1 - \beta z^{-1}} z^{-d}. \tag{17}$$

Therefore, the process pole $z = a_1$ no longer appears in the expression of $S(z)$, which guarantees internal stability. By using this expression, the controller can also be implemented in a two-degree-of-freedom (2DOF) control structure.

The above formulations allow an analysis of the control problem for UFOPDT models. Hereafter, attention is focused on the tuning rules problem with analysis of the sampling period and of the maximum multiplicative uncertainty. The tuning procedure of the controller for other orders, stable and integrative cases can be seen in [31,32].

3. Achievable robustness of the SDTC

In this section, the maximum achievable robustness produced by the SDTC for UFOPDT models is analyzed. Without loss of generality, the analysis is performed in the Laplace domain.

For this study, the following nominal process model

$$P_n(s) = G_n(s)e^{-L_n s} = \frac{b}{s-a}e^{-L_n s}, \tag{18}$$

is considered, where $G_n(s)$ is the delay-free model, b is a gain, a is the model pole, and L_n is the dead time. The feedback gain k is tuned to obtain the desired closed-loop pole p_c leading to

$$k = (a - p_c)/b. \tag{19}$$

In this analysis, a first order filter

$$V(s) = \frac{b_1 s + b_2}{s - \alpha_c} \tag{20}$$

is used, where b_1 and b_2 are the filter coefficients and α_c is a free tuning parameter. Hence, the filter $V(s)$ can be derived from the following two conditions as addressed in [31]

$$V(0) = k_r = k - a/b, \tag{21}$$

$$V(a) = k e^{L_n a}. \tag{22}$$

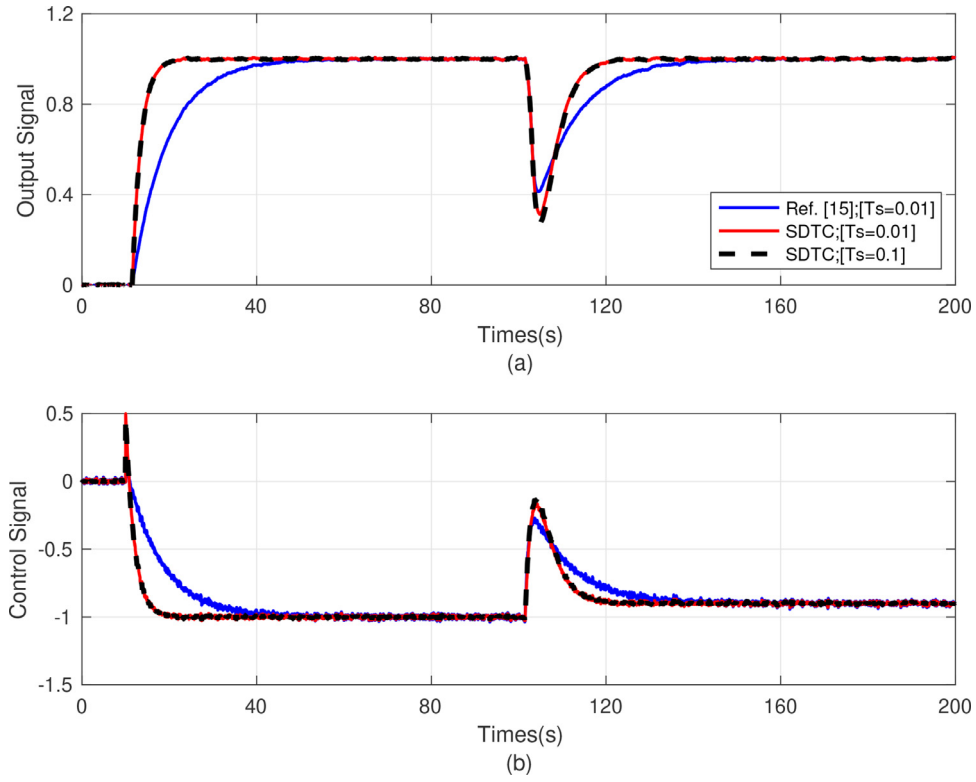

Fig. 7. Example 1: nominal closed-loop response.

Once having (20), (21) and (22), b_1 and b_2 are obtained

$$b_2 = \left(\frac{a}{b} - k\right)\alpha_c, \tag{23}$$

$$b_1 = \frac{k(a-\alpha_c)e^{L_n a} - b_2}{a}. \tag{24}$$

As stated in [31], there is a trade off between performance and robustness. So, to achieve the highest as possible robustness, the limit of the parameters α_c and p_c should tend to zero, thus, the following equations are derived

$$\lim_{p_c,\alpha_c \to 0} V(s) = \frac{a}{b}e^{L_n a}, \;\; k = \frac{a}{b}. \tag{25}$$

Using (5) and (25) the achievable robustness for the SDTC is obtained

$$I_r(\omega) = \frac{w}{ae^{L_n a}}, \;\; \omega > 0. \tag{26}$$

In DT processes, the most critical source of uncertainty is the related to the time delay [21]. Thus, for simplicity, the multiplicative uncertainty is given by

$$\delta P(\omega) = \frac{|P(j\omega) - P_n(j\omega)|}{|P_n(j\omega)|} = \left|e^{-\delta L j\omega} - 1\right|, \;\; \omega > 0 \tag{27}$$

where $\delta L = L - L_n$ and L represents the real process delay. An upper limit of $\delta P(\omega)$ can be defined as

$$\overline{\delta P}(\omega) = |\delta L|\omega \geq \delta P(\omega), \;\; \omega > 0. \tag{28}$$

According to (5), (26), and (28) the following robustness stability condition can be obtained

$$|\delta L| < \frac{1}{ae^{L_n a}} = \delta L_m, \tag{29}$$

where δL_m represents the maximum upper bound of the dead-time mismatch that an SDTC structure can stabilise.

The time delay uncertainty will now be defined as a fraction of the maximum upper bound of the dead-time-estimation error, such that

$$L = L_n + \delta L = L_n + \lambda.\delta L_m, \tag{30}$$

as can be seen from Eqs. (29) and (30) λ is within the range $0 < \lambda < 1$ to guarantee robust stability. In practice, it is not common to consider the dead time mismatch close to the achievable robustness. Therefore, in this work, λ is considered to be within the range [0.07 – 0.3] to include the most typical values of a dead-time mismatch from the literature [14,28,37].

4. Tuning rules of the robustness filter

In this section, tuning rules are proposed for the SDTC regarding open-loop unstable processes represented by UFOPDT models. The proposed tuning rules are obtained through several simulations considering the normalised model

$$P_n(s) = \frac{1}{s-1}e^{-L_n s}. \tag{31}$$

The main objective of the simulations is to tune the robustness filter for several scenarios, i.e., considering different nominal dead times L_n, desired closed-loop time constants $\tau_{cl} = 1/p_{cl}$, and maximum upper bounds λ within a desired range. Based on the obtained data, a new approach for the robustness filter tuning is proposed, as detailed in the following steps:

1. Set parameters L_n, τ_{cl}, and λ within the range [0.2 to 1.5], [1.3 to 2] and [0.07 to 0.3], respectively. These ranges were chosen to comprise the average works in literature.
2. Choose a data point $(L_n, \tau_{cl}, \lambda)$ from step 1.
3. Determine the feedback gain $k = (1 - 1/\tau_{cl})$ for the desired set-point tracking.
4. Gradually vary α_c until the minimum distance between $I_r(\omega)$ and $\delta P(w)$ is equal to 2 dB in order to obtain a robust

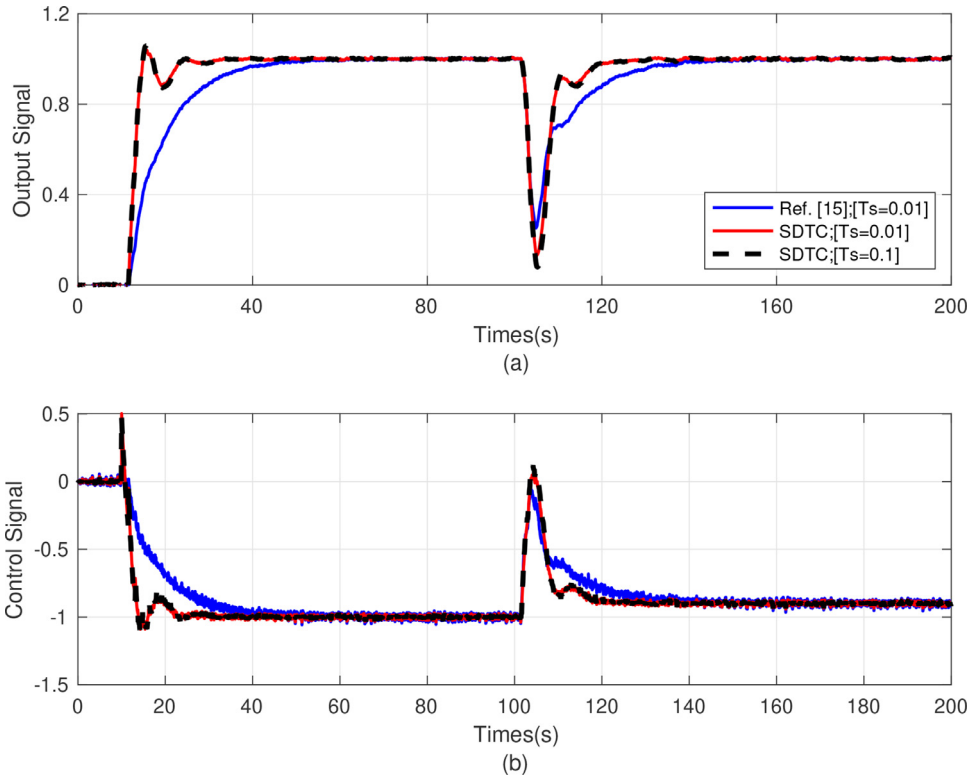

Fig. 8. Example 1: perturbed closed-loop response.

Table 1
Coefficients of the estimated function polynomial (32).

Coefficient	Value
p_0	1.2517
p_1	−1.2199
p_2	12.4692
p_3	−3.5003

stability margin. The numerator filter parameters b_2 and b_1 are calculated through (23) and (24), respectively.

5. Repeat steps 2–4 until the α_c for all data points are computed.
6. Estimate a function, using polynomial linear regression on the dataset, based on the polynomial

$$\hat{\alpha}_c = p_0 + p_1 \cdot L_n + p_2 \cdot \tau_{cl} + p_3 \cdot \lambda. \tag{32}$$

The coefficients of the estimated function polynomial are presented in Table 1.

7. Check the stability of all solutions, by testing $\hat{\alpha}_c$ in simulations for the full parameters range.
Results are detailed in Fig. 3, in which red and blue color represent the unstable and stable cases, respectively. The unstable restriction is overcome by doing

$$\lambda < 0.1 \cdot \tau_{cl} - 0.1 \cdot L_n + 0.3. \tag{33}$$

In such a way as to validate the proposed rule, it will be graphically compared with the dataset. The rule is obtained from a 4-D dataset, thus, to make possible the visualization in a 3-D chart, the parameter λ is fixed in 0.1. Fig. 4 represents the comparison of the filter tuning with the method from steps 2–5 and with the tuning rule, when $\lambda = 0.1$. The red dots indicate the $\hat{\alpha}_c$ values calculated according to (32).

As can be seen in (32), the data is approximated by a first-order polynomial function. A higher order approximation could obtain a better accuracy, but with a very small performance improvement to justify a rather complex polynomial.

Therefore, in this work, the estimated robustness parameter is given by

$$\hat{\alpha}_c = p_0 + p_1 \cdot L_n + p_2 \cdot \tau_{cl} + p_3 \cdot \lambda, \tag{34}$$

subject to: $\lambda < 0.1 \cdot \tau_{cl} - 0.1 \cdot L_n + 0.3$, where:

$$\begin{cases} 0.07 < \lambda < 0.3; \\ 1.3 < \tau_{cl} < 2; \\ 0.2 < L_n < 1.5. \end{cases} \tag{35}$$

5. Sampling period analysis

The choice of sampling period T_s is known to have a significant effect on the performance and robustness of a control system [35]. From the implementation perspective, it is interesting to choose the highest possible sampling period without compromising robustness and performance. As the implementation of DTC's is in the discrete-time domain, then, higher sampling periods imply simpler control algorithms. For instance, having a closed-loop DTC system with a delay of $L_n = 1.0$ (s) and a sampling period of $T_s = 0.01$ s would mean that at least 100 samples would have to be stored to compute the control signal at each sampling period. Therefore, in this work, the choice of the sampling period is performed by an graphical analysis for FOPDT models which considers the following normalized model.

$$G(s) = \frac{1}{s-1} e^{-L_n s}. \tag{36}$$

The graphical analysis of the sampling period is performed in the boundaries of the dead-time range defined in Section 4, which are $L_n = 1.5$ and $L_n = 0.2$, respectively.

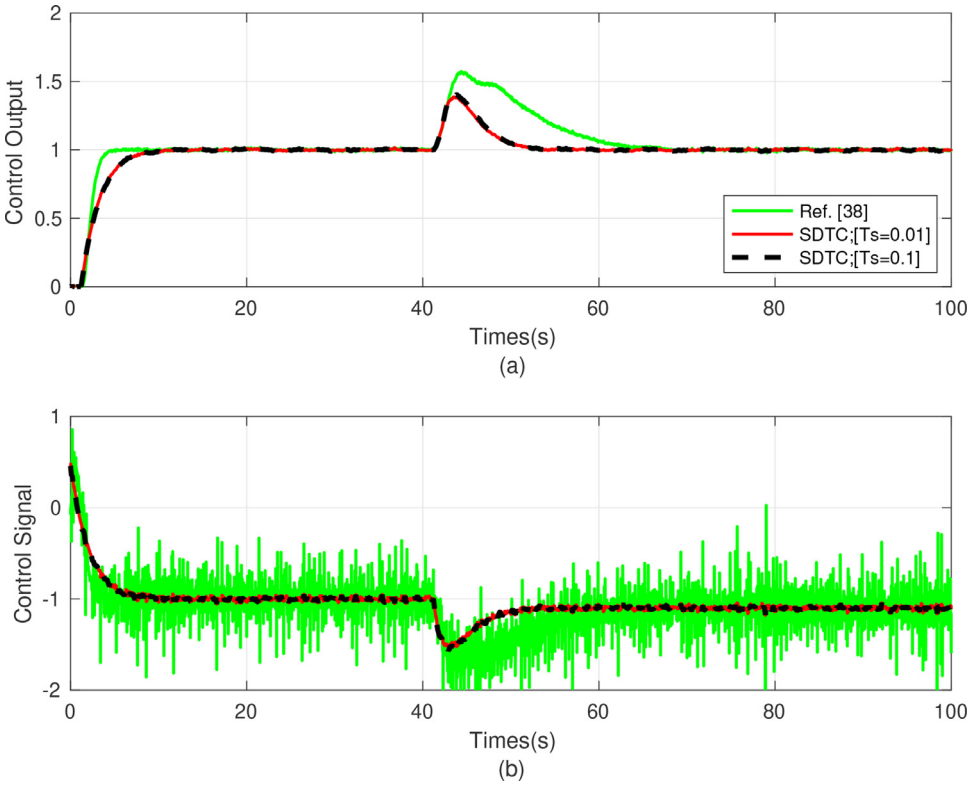

Fig. 9. Example 2: nominal closed-loop response.

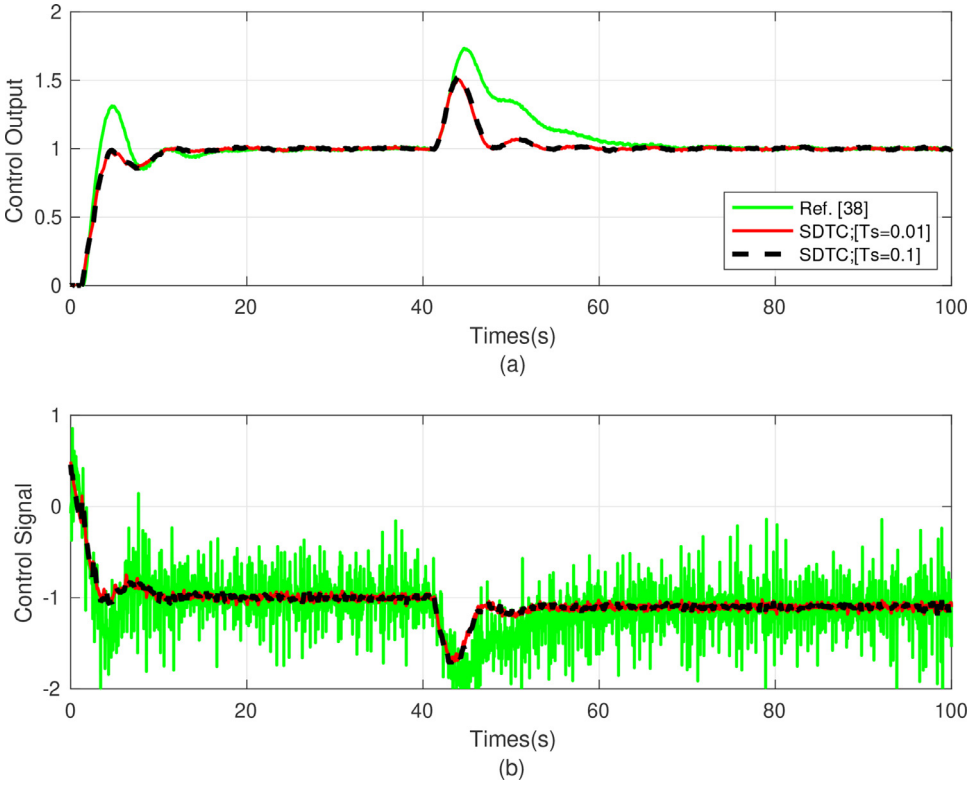

Fig. 10. Example 2: perturbed closed-loop response.

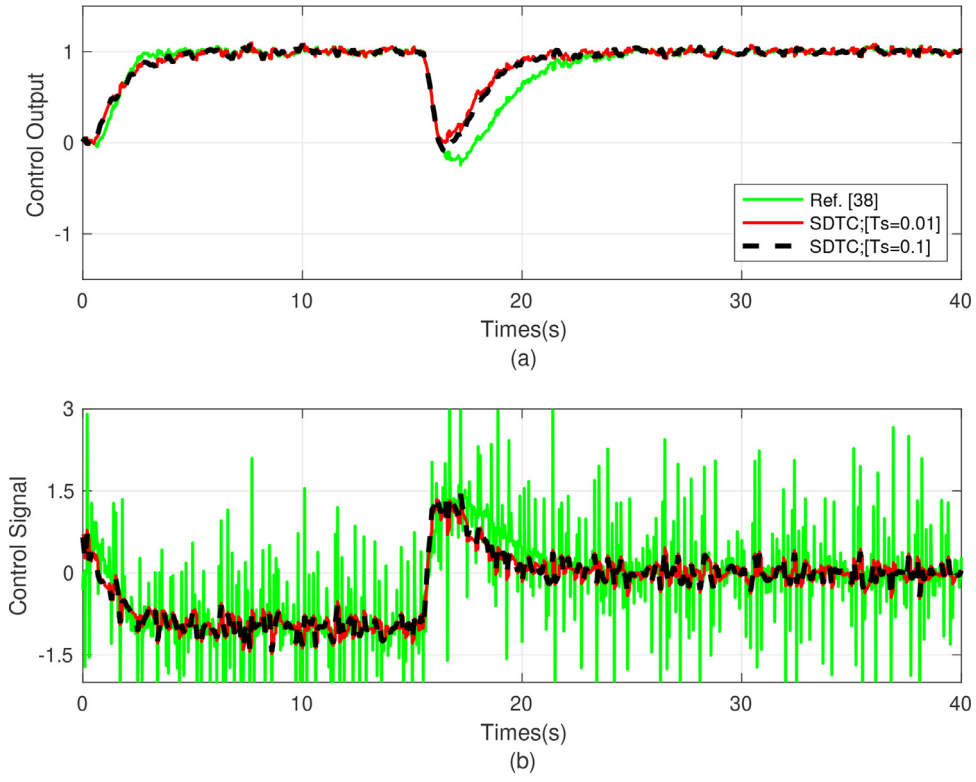

Fig. 11. Example 3: nominal closed-loop response.

Table 2
Performance comparison.

Example	$P_n(s)$	$P'_n(s)_{normalized}$	τ_{cl} [s]	L	δL (%)	δL_{max}
1	$\frac{1}{s-1}e^{-1.5s}$	–	2.01	1.5	5	0.2231
2	$\frac{1}{s-1}e^{-1.2s}$	–	1.303	1.2	10	0.3012
3	$\frac{1}{s-1}e^{-0.5s}$	–	1.303	0.5	20 and 50	0.6065
4	$\frac{3.433}{103.1s-1}e^{-20s}$	$\frac{3.433}{s-1}e^{-0.194s}$	0.2008	0.2	30	0.8237

Table 3
Controller parameters for example 1.

	$T_s = 0.01$	$T_s = 0.1$
$P_n(z)$	$\frac{0.01005}{z-1.01}z^{-150}$	$\frac{0.1052}{z-1.105}z^{-15}$
k	1.496	1.464
k_r	0.4963	0.4637
$V(z)$	$\frac{8.692-8.69z^{-1}}{1-0.9968z^{-1}}$	$\frac{8.396-8.382z^{-1}}{1-0.9683z^{-1}}$

5.1. Analysis for $L_n = 1.5$

Initially, the SDTC controller is designed using the tuning rule from (32) in Section 4. Thus, the closed-loop time constant is chosen: $\tau_{cl} = 2$, resulting $\hat{\alpha}_c = -0.3219$. This proposal considers a 30% of delay uncertainty compared to the maximum achievable robustness (see (29)), which means $\lambda = 0.3$. Secondly, an equivalent discrete-time controller is designed for the set of sampling periods $T_s = \{0.01,\ 0.02,\ 0.03,\ 0.05,\ 0.1,\ 0.25\}$ which are sub-multiples of L. Finally, in Fig. 5 are plotted the multiplicative uncertainty, the robustness index considering different sampling periods, and the shortest dead-time multiplicative uncertainty $\overline{\delta P}$ that violates the robustness stability condition (28) for the set of sampling periods.

Considering the same security margin, i.e. the minimum distance between δP and the I_R curve, Fig. 5 is generated including a range of sampling periods. Then, making the security margin be zero, $\overline{\delta P}$ is obtained. Note that the security margin, which can be measured at the critical frequency ω_c [35], remains constant for sampling period $T_s \leq 0.1$.

As expected, the curves of I_R present the same gain at medium and low frequencies. Nevertheless, there is a gain reduction near to frequency π/T_s. This behaviour, in practice, does not compromise the achievable robustness for the set of controllers and sampling periods, only the controller with $T_s = 0.25$ presented an achievable robustness reduction.

Besides, it is important to highlight that the lowest frequency where $\overline{\delta P}$ achieves the maximum gain is $\omega_m = \pi/\overline{\delta L}$, thus, through a graphical analysis from Fig. 5, it can be seen that the sampling period must obey the following condition

$$\frac{\pi}{T_s} > \frac{\pi}{\overline{\delta L}} = \omega_m, \tag{37}$$

which is equivalent to

$$T_s < \overline{\delta L} = 0.1069. \tag{38}$$

Therefore, the final choice of sampling period must satisfy (38) and T_s must be a sub-multiple of L. From this analysis the best choice is $T_s = 0.1$, in accordance with the graphical analysis.

Afterwards, a similar analysis is performed for $L_n = 0.2$.

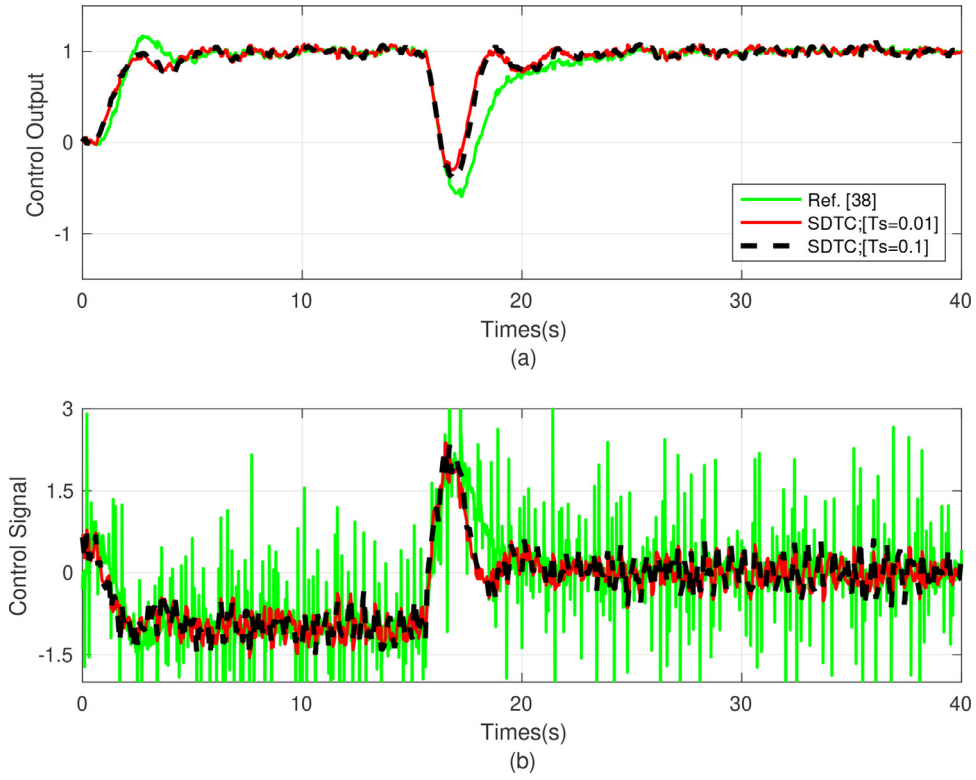

Fig. 12. Example 3: perturbed closed-loop response.

Table 4
Controller parameters for example 2.

	$T_s = 0.01$	$T_s = 0.1$
$P_n(z)$	$\frac{0.01005}{z-1.01} z^{-120}$	$\frac{0.1052}{z-1.105} z^{-12}$
k	1.496	1.464
k_r	0.4963	0.4637
$V(z)$	$\frac{8.06-8.057z^{-1}}{1-0.993z^{-1}}$	$\frac{7.676-7.644z^{-1}}{1-0.9326z^{-1}}$

Table 5
Controller parameters for example 3.

	$T_s = 0.01$	$T_s = 0.1$
$P_n(z)$	$\frac{0.01005}{z-1.01} z^{-50}$	$\frac{0.1052}{z-1.105} z^{-5}$
k	1.762	1.704
k_r	0.7625	0.7040
$V(z)$	$\frac{7.059-7.044z^{-1}}{1-0.9805z^{-1}}$	$\frac{6.383-6.258z^{-1}}{1-0.8215z^{-1}}$

Table 6
Controller parameters for example 4.

	$T_s = 0.5$	$T_s = 5$
$P_n(z)$	$\frac{0.01702}{z-1.005} z^{-40}$	$\frac{0.01741}{z-1.051} z^{-4}$
k	1.742	1.562
k_r	1.4506	1.2709
$V(z)$	$\frac{3.787-3.769z^{-1}}{1-0.9877z^{-1}}$	$\frac{3.354-3.206z^{-1}}{1-0.8839z^{-1}}$

5.2. Analysis for $L_n = 0.2$

In this case, the SDTC closed-loop pole is the same as in the previous example ($\tau_{cl} = 2$), then, using Eq. (32), the filter pole is computed as $\hat{\alpha}_c = -1.0952$.

To perform the analysis, equivalent discrete-time controllers considering the set $T_s = \{0.01,\ 0.02,\ 0.04,\ 0.05,\ 0.1,\ 0.2\}$ are chosen. In Fig. 6 are plotted δP considering 30% of uncertainty ($\lambda = 0.3$), the maximum achievable robustness, $\overline{\delta P}$, and the robustness index for the set of sampling periods. As evidenced in Fig. 6, the proposed controller has the same achievable robustness for all set of sampling periods.

Following the condition established by (38), in this case, the condition would be

$$T_s < \overline{\delta L} = 0.3006. \tag{39}$$

However, as previously shown in the analysis of Figs 5 and 6, for simplicity, it is assumed that the sampling period is submultiple of the nominal dead time L_n. Thus the chosen sampling period must satisfy

$$T_s < \min(\overline{\delta L}, L_n). \tag{40}$$

6. Simulation results

In order to validate the tuning rules, comparative examples commonly used in the literature considering UFOPDT processes are presented in Table 2.

To achieve a disturbance rejection response faster than the open-loop dynamics, the robustness filter was tuned according to the rule present in (32) and the sampling period was chosen as presented in Section 5.

For each example, it has been performed simulations with and without noise. Besides, for a fair comparison, the same noise is added for each example. In this work, only the noise simulation figures are illustrated, as the noise does not significantly impact the dynamics of the responses.

The performance indices Integral Absolute Error (IAE), Total Variation (TV), and the cost function J for all examples are calculated only for input disturbance rejection response and presented in Tables 7 and 8. These indices are defined as follows

$$\text{IAE} = \int_0^\infty |e(t)|dt, \tag{41}$$

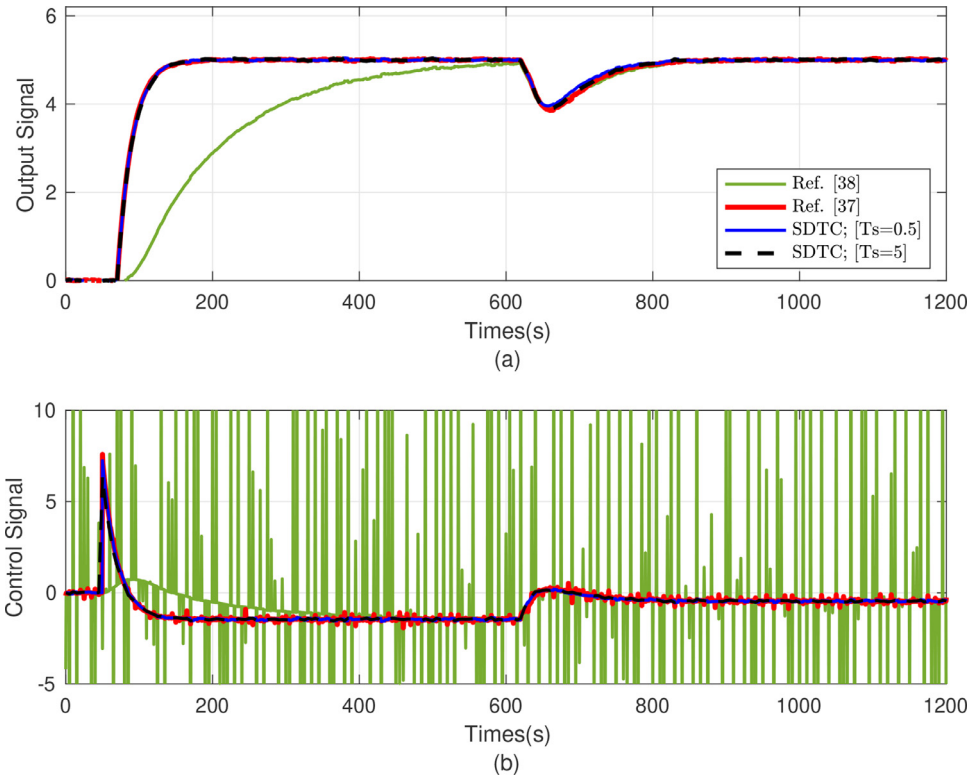

Fig. 13. Example 4: nominal closed-loop response.

Table 7
Performance indices for non-noisy simulation examples. The two best cases are highlighted in bold text.

Example		Nominal			Perturbed		
		IAE	TV	J	IAE	TV	J
Example 1	SDTC [$T_s = 0.01$]	4.79	1.54	6.6	4.79	2.09	9.1
	SDTC [$T_s = 0.1$]	**5.05**	1.61	**7.3**	**5.04**	2.30	**10.9**
	Ref. [28] [$T_s = 0.01$]	6.86	**1.31**	8.1	6.85	**2.09**	12.5
Example 2	SDTC [$T_s = 0.01$]	**1.87**	**0.94**	**0.5**	**1.87**	**1.56**	**2.7**
	SDTC [$T_s = 0.1$]	**1.98**	**0.99**	**0.5**	**2.01**	**1.77**	**2.9**
	Ref. [14]	5.89	2.38	13.1	5.86	2.77	13.9
Example 3	SDTC [$T_s = 0.01$]	**2.44**	**3.48**	**2.7**	**2.44**	**6.97**	**12.1**
	SDTC [$T_s = 0.1$]	**2.67**	**3.70**	**3.3**	**2.76**	8.28	15.6
	Ref. [14]	4.27	3.81	10.4	4.26	**5.27**	**13.6**
Example 4	SDTC [$T_s = 0.5$]	**68.72**	**2.29**	**167.5**	**88.29**	4.10	**346.4**
	SDTC [$T_s = 5$]	**76.25**	2.42	**197.4**	**100.13**	4.43	**367.2**
	Ref. [37] [$T_s = 0.5$]	101.11	**2.37**	226.8	101.21	**3.92**	402.9
	Ref. [14]	110.27	2.55	342.1	110.54	**3.63**	536.8

$$\mathrm{TV} = \sum_{i=1}^{\infty} |u_{i+1} - u_i|, \tag{42}$$

$$\mathrm{J} = J_1 + J_2, \tag{43}$$

where

$$J_1 = \mathrm{IAE} \cdot \sum_{i=1}^{\infty} |y_{i+1} - y_i|, \tag{44}$$

$$J_2 = \mathrm{IAE} \cdot \left(\sum_{i=1}^{\infty} |u_{i+1} - u_i| - |2u_m - u_\infty - u_0| \right), \tag{45}$$

u_0 is the initial value, u_∞ is the final value, and u_m is the most extreme value of the control signal.

All the simulations herein are carried out using a continuous-time process plant, while the designed controllers are discrete-time transfer functions. In Tables 7 and 8, the two best cases are highlighted in bold text.

6.1. Example 1

The proposed controller is compared with one recently studied in [28], which consist in a SP generalisation. The model used for simulations is the first one presented in Table 2, such as

$$P_n(s) = \frac{1}{s-1} e^{-1.5s}. \tag{46}$$

This system is remarked as rather challenging due to its long delay [26,28].

The SDTC is tuned according to the proposed rules for $\lambda = 0.3$. For the purpose of comparing the sampling period analysis described in Section 5, it will be used the sampling period given by [28], $T_s = 0.01$ s, and the achieved by the proposed strategy,

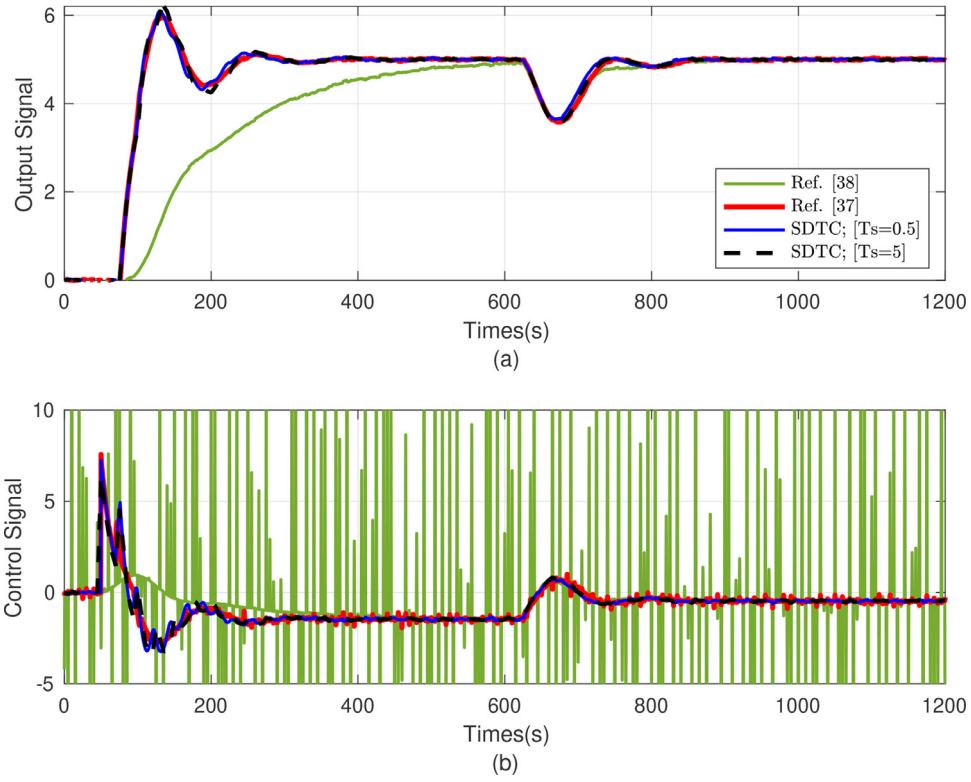

Fig. 14. Example 4: perturbed closed-loop response.

Table 8
Performance indices for noisy simulation examples. The two best cases are highlighted in bold text.

Example		Nominal			Perturbed		
		IAE	TV	J	IAE	TV	J
Example 1	SDTC [$T_s = 0.01$]	**4.89**	**10.05**	**59.8**	**4.90**	**15.23**	**70.6**
	SDTC [$T_s = 0.1$]	**5.15**	**9.17**	**61.7**	**5.16**	**12.11**	**79.8**
	Ref. [28] [$T_s = 0.01$]	6.90	12.79	107.2	6.91	23.27	142.7
Example 2	SDTC [$T_s = 0.01$]	**0.95**	**38.04**	**53.8**	**2.01**	**17.65**	**41.5**
	SDTC [$T_s = 0.1$]	**1.04**	**29.75**	**49.4**	**2.14**	**13.08**	**45.7**
	Ref. [14]	5.93	288.96	1579.4	5.88	266.43	1654.5
Example 3	SDTC [$T_s = 0.01$]	**1.98**	**82.70**	**225.9**	**2.77**	**68.44**	**216.5**
	SDTC [$T_s = 0.1$]	**2.17**	**64.23**	**209.9**	**3.06**	**56.78**	**261.5**
	Ref. [14]	4.46	382.75	1919.7	4.45	406.81	1915.7
Example 4	SDTC [$T_s = 0.5$]	**88.20**	**5.69**	**683.5**	**89.24**	**8.44**	**882.8**
	SDTC [$T_s = 5$]	**97.37**	**5.01**	**724.8**	**100.22**	**7.42**	**984.5**
	Ref. [37] [$T_s = 0.5$]	101.94	31.54	3591.9	102.13	35.70	3619.8
	Ref. [14]	110.72	1945.2	273120.0	110.67	1948.3	27402.0

$T_s = 0.1$ s. The obtained discrete model and the controller parameters for each sampling period are listed in Table 3. For all examples, gains k and k_r were calculated according to (7) and (8), respectively. The robustness filter parameter $\hat{\alpha}_c$ was obtained using (32).

Fig. 7 presents the results for the nominal case and Fig. 8 for the case with uncertainty. The simulations show the proposed controller response using both sampling periods, $T_s = 0.01$ s and $T_s = 0.1$ s, compared to the controller response from reference [28]. A unity step-change is applied at time $t = 10$ s and a negative constant load disturbance of magnitude 0.1 was added to the the control signal at time $t = 100$ s.

As can be seen from Figs 7 and 8, using either $T_s = 0.01$ or $T_s = 0.1$, both SDTCs get similar responses. This allows using a larger sampling period without compromising the performance significantly. The IAE, TV and J are computed considering the simulations data from 90 s to 180 s. The SDTC presented better IAE and J for both nominal and uncertainty cases, as can be seen in Tables 7 and 8. However, both SDTCs presented faster disturbance rejection, consequently higher TV, in the noise free case.

6.2. Example 2

Consider the following example [14]

$$P_n(s) = \frac{1}{s-1}e^{-1.2s}. \tag{47}$$

The process discrete model and the controller parameters with sampling period $T_s = 0.1$ s and $T_s = 0.01$ s using $\lambda = 0.3$ are given by Table 4.

For comparative purposes, it was used a recent continuous-time controller studied in [14]. Fig. 9 illustrates the results for the nominal case and Fig. 10 for the perturbed case. A unit step change in the set point starts at $t = 0$ s and a step change disturbance of magnitude 0.1 was introduced at $t = 40$ s.

It can be seen from Figs 9 and 10 that the SDTCs presented faster disturbance rejection, smaller cost function, and better noise

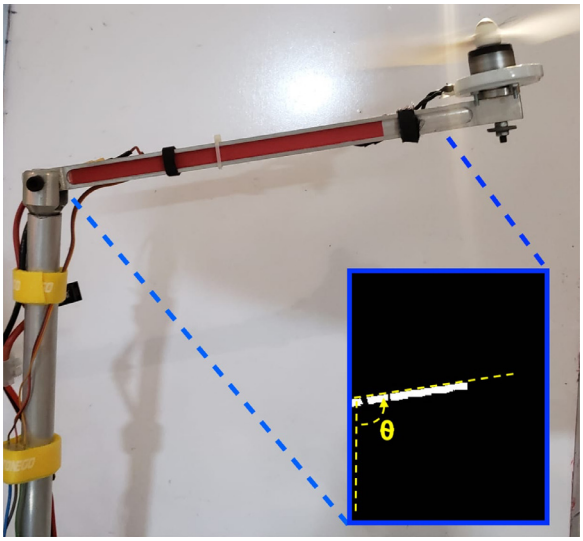

Fig. 15. The propeller pendulum.

attenuation even with a more aggressive tuning, leading to better results for all performance indices, as can be seen in Tables 7 and 8.

6.3. Example 3

Consider another process studied in [14]

$$P_n(s) = \frac{1}{s-1}e^{-0.5s}. \tag{48}$$

The process discrete-time models with sampling period $T_s = 0.01\ s$ and $T_s = 0.1\ s$ using $\lambda = 0.2$ are given by

Simulation results for nominal and with uncertainty case are shown in Figs 11 and 12, respectively. For this simulation, an unit step change is added to the set-point at $t = 0$ s and a negative unit step load disturbance is applied to the process input at $t = 15$ s.

The SDTC presented faster disturbance rejection and better performance indexes for all the scenarios in the nominal case, as can be seen in Tables 7 and 8. The perturbed case presented better indices, except for the TV and J of the noise-free case. Also, note that in the noisy case, the SDTCs present better noise attenuation in terms of TV, even with a first-order robustness filter, because the control structure of [14] does not present a solution to deal with measurement noise.

6.4. Example 4

The chemical reactor concentration control problem that was also studied in many works, such is [14,33,37], will be analyzed in this case study. The model is given by

$$P_n(s) = \frac{3.433}{101.1s-1}e^{-20s}, \tag{49}$$

and the normalized model from Table 2

$$P'_n(s) = \frac{3.433}{s-1}e^{-0.194s}. \tag{50}$$

The process discrete model with sampling period $T_s = 0.5\ s$ and $T_s = 5\ s$ using $\lambda = 0.08$ is given by

The SDTCs were compared with both references [14,37]. Results are shown in Figs 13 and 14 for nominal and with uncertainty case, respectively. For comparison, a step change with magnitude 5 is added to the set-point at $t = 50\ s$ and a negative unity step change is applied to the process at $t = 600$ s.

It can be noted from Tables 7 and 8 that the proposed strategy has a better load disturbance response in terms of IAE for both noisy and non-noisy cases and, in the noisy case, better noise attenuation in terms of TV, with a bigger difference compared to the controller from Ref. [14]. Also, for all cases, SDTC presented smaller cost function. Considering the twelve scenarios, the SDTCs had better indices in ten of them. The exception was the TV from the noise-free cases, due to the more aggressive tuning of the SDTCs.

7. Experimental results

In this section, an in-house developed propeller pendulum, shown in Fig. 15, is used to validate both the proposed tuning rule and the method of choosing the sampling period. The propeller pendulum is a nonlinear system, and its dynamics varies according to the angle θ. In this work, the control objective is to control the angular position when the angle θ is bigger than 90° at steady-state, precisely, when the open-loop dynamic is unstable [10].

Fig. 16 shows a simplified diagram of the developed system. As can be seen, the system consists of an arm with a propeller (actuator) to rotate the arm angle. The input is the propeller motor voltage, and the output is the angular arm position. For simplicity, the input is normalised between the range $[-1,\ 1]$. The output, that is, the angular arm position, is estimated using a video camera and an image processing algorithm. The control strategy is implemented in a computer and, through a dedicated wi-fi network, it receives and sends the output measurements and the control signal, respectively.

The pendulum model can be obtained using a phenomenological analysis or though identification methods. In this case, the second approach is used, so that, considering the operation point of 110°, the following model is obtained.

$$P_n(s) = \frac{4.066}{11.11s-1}e^{-3s}. \tag{51}$$

Observe that the dead time is originated mainly by the accumulation of time lags from a series of processes, like the video capture, image processing, network communication, and high-order dynamics that are not modelled.

The normalised model is then given by

$$P'_n(s)_{normalised} = \frac{4.066}{s-1}e^{-0.27s}. \tag{52}$$

By using $\tau_{cl} = 2,\ \lambda = 0.2,$ and (32), it results $\alpha_c = -0.5043$.

Through identification experiments the maximum dead-time uncertainty was estimated as $\overline{\delta L} = 1.4\ s$. By using condition (40), where $T_s < \min(\overline{\delta L} = 1.4, L_n = 3)$, T_s can be chosen in the set $T_s = \{0.15,\ 0.3,\ 0.6,\ 1\}\ s$. Therefore, the sampling period was chosen as $T_s = 1\ s$ and the discrete-time model of the process results as

$$P_n(z) = \frac{0.383z^{-1}}{1-1.094z^{-1}}z^{-3}. \tag{53}$$

Considering the tuning parameters and model (53), the SDTC results then with $k = 1.273,\ k_r = 1.0275$ and robustness filter

$$V(z) = \frac{4.362-3.955z^{-1}}{1-0.604z^{-1}}. \tag{54}$$

The experiment was performed with a set-point step change of 20° at $t = 20s$ and a step disturbance of 0.5 added to the control signal at $t = 100s$.

The results can be seen in Fig. 17. Although the system is nonlinear and has modeling uncertainties involved, the controller successfully stabilises the system, tracks the set-point, and properly rejects the step load disturbance. Therefore, the experiment shows that the proposed tuning rule and the method for sampling period choice can be used to control a real unstable delayed process subjected to noise and uncertainties.

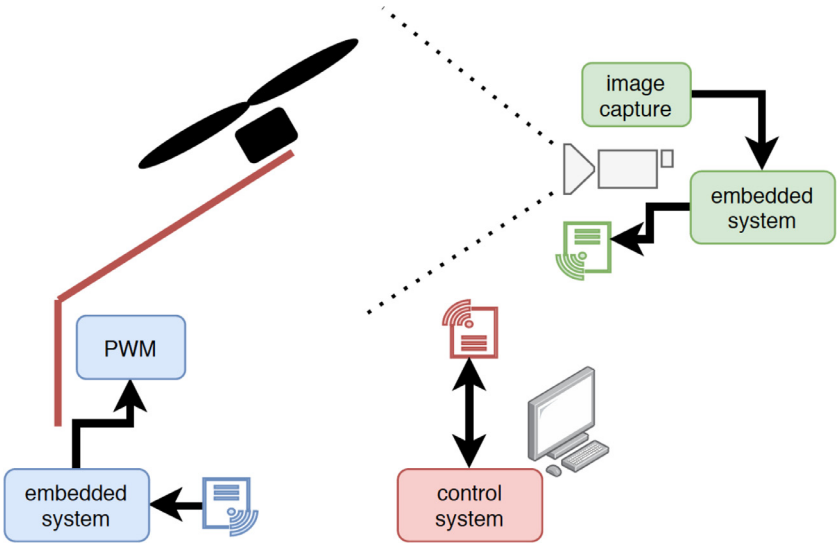

Fig. 16. Propeller pendulum control system.

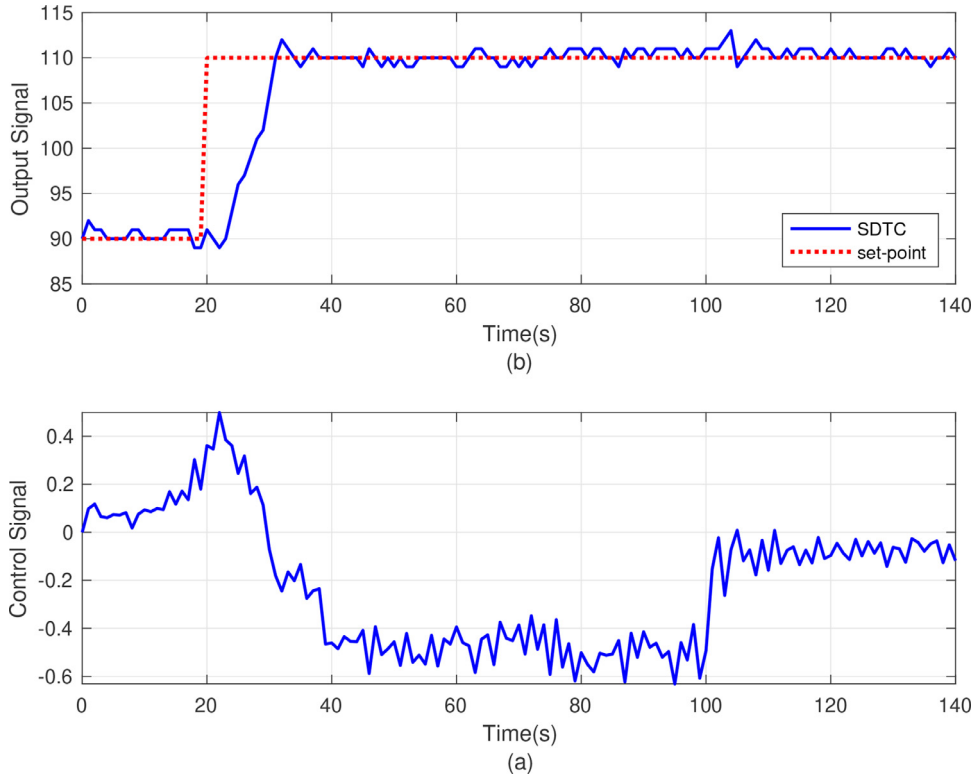

Fig. 17. Output and control signal responses of the experiment.

8. Conclusion

This work proposed new tuning rules for the SDTC applied to UFOPDT processes. The proposal guarantees robustness for processes with a wide range of nominal time delays, dead-time uncertainty, and desired closed-loop dynamics. As the SDTC implementation is done in the discrete-time domain, then it is also proposed a methodology for a proper choice of the sampling period, which is highly desirable to be the biggest as possible but without affecting the performance and robustness significantly. This is useful in industrial applications to save network resources.

The effectiveness of the proposal can be observed through simulation and experimental results. From the simulations, the new tuning rules allowed the SDTC to provide better or equivalent results for disturbance rejection when compared to recent works. In addition, it was possible to use sampling periods ten times larger than the other discrete controllers used for comparison, attaining performance close to or better than other controllers in the literature. The experiment showed that both proposed strategies presented good performance and robustness, even when it is applied to a nonlinear system with several uncertainties involved.

Declaration of Competing Interest

The authors declare that they have no known competing financial interests or personal relationships that could have appeared to influence the work reported in this paper.

Acknowledgments

The financial support from the Brazilian funding agencies CAPES, CNPq, FUNCAP, and Energia Pecem / ANEEL under the grant number PD-07267-0016/2018.

References

[1] P. Albertos, P. Garcia, Robust control design for long time-delay systems, J. Process Control 19 (10) (2009) 1640–1648.
[2] R. Farkh, K. Laabidi, M. Ksouri, Stabilizing sets of PI/PID controllers for unstable second order delay system, Int. J. Autom. Comput. 11 (2) (2014) 210–222.
[3] P. García, P. Albertos, Robust tuning of a generalized predictor-based controller for integrating and unstable systems with long time-delay, J. Process Control 23 (8) (2013) 1205–1216.
[4] P. García, P. Albertos, T. Hägglund, Control of unstable non-minimum-phase delayed systems, J. Process Control 16 (10) (2006) 1099–1111.
[5] A. González, A. Cuenca, V. Balaguer, P. García, Event-triggered predictor-based control with gain-scheduling and extended state observer for networked control systems, Inf. Sci. 491 (2019) 90–108.
[6] M. Huba, Some practical issues in the Smith predictor design for FOTD systems, in: Proceedings of the 2017 Forth International Conference on Control, Decision and Information Technologies (CoDIT), 2017, pp. 353–358.
[7] M. Huba, I. Bélai, Limits of a simplified controller design based on integral plus dead time models, Proc. Inst. Mech. Eng. I: J. Syst. Control Eng. 232 (6) (2018) 728–741.
[8] M. Huba, M. Halas, New filtered Smith predictors for FOPDT plants. Part I. First order disturbance filter, in: ERK 2010 – Devetnajsta mednarodna Elektrotehniska in racunalniska konferenca, IEEE, 2010a, pp. 339–342.
[9] M. Huba, M. Halas, New filtered Smith predictors for FOPDT plants. Part II. Second order disturbance filter, in: ERK 2010 – Devetnajsta mednarodna Elektrotehniska in racunalniska konferenca, IEEE, 2010b, pp. 343–345.
[10] M. Huba, T. Malatinec, T. Huba, Preparatory laboratory experiments for robust constrained UAVs control, IFAC Proc. Vol. 46 (17) (2013) 262–267. 10th IFAC Symposium Advances in Control Education
[11] M. Huba, P. Ťapák, Experimenting with the modified filtered Smith predictors for FOPDT plants, IFAC Proc. Vol. 44 (1) (2011b) 2452–2457. 18th IFAC World Congress
[12] M. Huba, P. Ťapák, Modified filtered Smith predictors for FOPDT plants, in: M. Huba, S. Skogestad, M. Fikar, M. Hovd, T. Johansen, B. Roháľllkiv (Eds.), Preprints of the Workshop "Selected topics on constrained and nonlinear control", STU Bratislava – NTNU Trondheim, 2011a, pp. 185–191.
[13] M. Huba, P. Kuĭha, K. Žákova, Observer-based control of unstable process with dead time, in: Proceedings of the Tenth Conference Process Control, 1, 1995, pp. 35–38.
[14] M.P. Kumar, K.V.L. Narayana, Multi control scheme with modified Smith predictor for unstable first order plus time delay system, Ain Shams Eng. J. 9 (4) (2018) 2859–2869.
[15] T.A. Lima, M.P. de Almeida Filho, B.C. Torrico, F.G. Nogueira, W.B. Correia, A practical solution for the control of time-delayed and delay-free systems with saturating actuators, Eur. J. Control 51 (2020) 53–64.
[16] V. Léchappé, E. Moulay, F. Plestan, Q.-L. Han, Discrete predictor-based event-triggered control of networked control systems, Automatica 107 (2019) 281–288.
[17] M.S. Mahmoud, Y. Xia, Chapter 2 – networked control systems' fundamentals, in: M.S. Mahmoud, Y. Xia (Eds.), Networked Control Systems, Butterworth-Heinemann, 2019, pp. 37–89.
[18] H. Manum, Extensions of Skogestad's SIMC tuning rules to oscillatory and unstable processes, Technical Report, 2006.
[19] M.R. Mataušek, T.B. Šekara, PID controller frequency-domain tuning for stable, integrating and unstable processes, including dead-time, J. Process Control 21 (1) (2011) 17–27.
[20] M.M. Morato, J.E. Normey-Rico, A linear parameter varying approach for robust dead-time compensation, IFAC-PapersOnLine 52 (1) (2019) 880–885. 12th IFAC Symposium on Dynamics and Control of Process Systems, including Biosystems DYCOPS 2019
[21] J.E. Normey-Rico, E.F. Camacho, Control of dead-time processes, Springer, Berlin, 2007.
[22] J.E. Normey-Rico, E.F. Camacho, Dead-time compensators: a survey, Control Eng. Pract. 16 (4) (2008) 407–428.
[23] J.E. Normey-Rico, E.F. Camacho, Unified approach for robust dead-time compensator design, J. Process Control 19 (1) (2009) 38–47.
[24] J.E. Normey-Rico, R. Sartori, M. Veronesi, A. Visioli, An automatic tuning methodology for a unified dead-time compensator, Control Eng. Pract. 27 (2014) 11–22.
[25] F. Padula, A. Visioli, Optimal tuning rules for proportional-integral-derivative and fractional-order proportional-integral-derivative controllers for integral and unstable processes, IET Control Theory Appl. 6 (6) (2012) 776–786.
[26] Y.Z. Qing-Guo Wang Han-Qin Zhou, Y. Zhang, A comparative study on control of unstable processes with time delay, in: Proceedings of the 2004 Fifth Asian Control Conference (IEEE Cat. No.04EX904), 3, 2004, pp. 1996–2004Vol.3.
[27] T.L. Santos, P.E. Botura, J.E. Normey-Rico, Dealing with noise in unstable dead–time process control, J. Process Control 20 (7) (2010) 840–847.
[28] R. Sanz, P. García, P. Albertos, A generalized smith predictor for unstable time-delay SISO systems, ISA Trans. 72 (2018) 197–204.
[29] O.J.M. Smith, Closer control of loops with dead time, Chem. Eng. Prog. 53 (5) (1957) 217–219.
[30] R.P. Sree, M. Chidambaram, Control of unstable bioreactor with dominant unstable zero, Chem. Biochem. Eng. Q. 17 (2003) 139–145.
[31] B.C. Torrico, M.P. de Almeida Filho, T.A. Lima, M.D. do N. Forte, R.C. Sá, F.G. Nogueira, Tuning of a dead-time compensator focusing on industrial processes, ISA Trans. 83 (2018) 189–198.
[32] B.C. Torrico, M.P. de Almeida Filho, T.A. Lima, T.L. Santos, F.G. Nogueira, New simple approach for enhanced rejection of unknown disturbances in LTI systems with input delay, ISA Trans. 94 (2019) 316–325.
[33] B.C. Torrico, M.U. Cavalcante, A.P.S. Braga, A.A.M. Albuquerque, J.E. Normey-Rico, Simple tuning rules for dead-time compensation of stable, integrative, and unstable first-order dead-time processes, Ind. Eng. Chem. Res. 52 (2013) 11646–11654.
[34] B.C. Torrico, W.B. Correia, F.G. Nogueira, Simplified dead-time compensator for multiple delay SISO systems, ISA Trans. 60 (2016) 254–261.
[35] B.C. Torrico, J.E. Normey-Rico, 2DOF discrete dead-time compensators for stable and integrative processes with dead-time, J. Process Control 15 (3) (2005) 341–352.
[36] B. Verma, P.K. Padhy, Robust fine tuning of optimal PID controller with guaranteed robustness, IEEE Trans. Ind. Electron. (2019) 1.
[37] D. Wang, T. Liu, X. Sun, C. Zhong, Discrete-time domain two-degree-of-freedom control design for integrating and unstable processes with time delay, ISA Trans. 63 (2016) 121–132.
[38] Z. Wang, H. Tian, X. Geng, J. Cui, T. Liu, Predictor based 2DOF control design for inverse response processes with time delay, in: Proceedings of the 2018 Thirty-third Youth Academic Annual Conference of Chinese Association of Automation (YAC), 2018, pp. 65–70.
[39] K. Watanabe, M. Ito, A process-model control for linear systems with delay, IEEE Trans. Autom. Control 26 (6) (1981) 1261–1269.
[40] P. Ťapák, M. Huba, Experimenting with modified Smith predictors using B&R automation studio target for simulink, IFAC Proc. Vol. 45 (7) (2012) 366–371. 11th IFAC, IEEE International Conference on Programmable Devices and Embedded Systems